Thesis for the degree of Licentiate of Engineering

Ionic Liquid Based Electrolytes for High-Temperature Lithium-Ion Batteries

Manfred Kerner

CHALMERS

Department of Applied Physics
Chalmers University of Technology
Göteborg, Sweden 2015

Ionic Liquid Based Electrolytes for High-Temperature Lithium-Ion Batteries
Manfred Kerner

Cover: HT-LIB, Li^+ coordinated by two TFSI

Department of Applied Physics
Chalmers University of Technology
SE-41296 Göteborg, Sweden

Chalmers, Reproservice
Göteborg, Sweden 2015

Ionic Liquid Based Electrolytes for High-Temperature Lithium-Ion Batteries

Manfred Kerner
Department of Applied Physics
Chalmers University of Technology
SE-41296 Göteborg, Sweden

Abstract

Today, lithium-ion batteries (LIBs) are ubiquitous in mobile phones, laptops, and other portable devices. The research community strives to further improve the LIB to increase electric driving distance and efficiency of both hybrid electric vehicles (HEVs) and fully electric vehicles (EVs). Conventional LIBs need to be strictly temperature controlled, most often cooled, to *ca*. 30°C, to ensure an acceptable and predictable life-time. Increasing the thermal stability and hence making possible operating temperatures of up to *ca*. 100°C would enable a merging of the cooling systems of the LIB and the power electronics – resulting in an overall reduced system complexity, saved mass, and a higher energy efficiency.

All components of the LIB must be thermally stable to deliver the targeted performance and life-time. The electrolytes of conventional LIBs all contain organic solvents and lithium salts, the former flammable with high vapour pressures and the latter meta-stable at room temperature and unstable at temperatures above 60°C. Thus more stable solvents and salts are needed to improve the inherent safety of the electrolyte – especially if aiming at elevated operating temperatures.

In this thesis one possible alternative is investigated in the form of ionic liquid (IL) based electrolytes. ILs often exhibit properties advantageous for electrolytes: low vapour pressures, high thermal stabilities, low flammabilities, and high ionic conductivities. The physico-chemical properties of several IL based electrolytes have been assessed and furthermore a detailed characterization of several commercial sources of an often used electrolyte Li-salt has been performed.

Keywords: lithium-ion battery, ionic liquid, electrolyte, LiFSI, high-temperature stability, EMITFSI, EMIFSI

List of Publications

This thesis is based on the work contained in the following papers:

I. Ionic liquid based lithium battery electrolytes: Fundamental benefits of utilizing both TFSI and FSI anions?
Manfred Kerner, Nareerat Plylahan, Johan Scheers, and Patrik Johansson
Physical Chemistry Chemical Physics, 2015, 17, 19569-19581.

II. Thermal stability and decomposition of lithium bis(fluorosulfonyl)imide (LiFSI) salts
Manfred Kerner, Johan Scheers, and Patrik Johansson
Submitted

Contribution Report

I. I performed all the measurements and data analysis – with the exception of the LSV measurements and simulation of Raman spectra. I was the main author of the paper.

II. I performed all the measurements and data analysis and was the main author of the manuscript.

Table of Contents

List of Figures

List of Acronyms

DMAc	Dimethylacetamide
DMC	Dimethyl carbonate
DSC	Differential scanning calorimetry
EMI	1-ethyl-3-methyl-imidazolium
EMC	Ethyl methyl carbonate
ESW	Electrochemical stability window
EV	Electric vehicle
FSI	Bis(fluorosulfonyl)imide
FTFSI	(Fluorosulfonyl) (trifluoromethanesulfonyl)imide
FT-IR	Fourier transform infrared
HEV	Hybrid electric vehicle
HT-LIB	High-temperature LIB
IL	Ionic liquid
LIB	Lithium-ion battery
LiBOB	Lithium bis(oxalato)borate
MS	Mass spectrometer
NiCd	Nickel-cadmium
NiMH	Nickel-metal-hydride
OCV	Open circuit voltage
PC	Propylene carbonate
Pyr	Pyrrolidinium
SEI	Solid electrolyte interphase
SLI	Starting, lighting, ignition
TFSI	Bis(trifluoromethanesulfonyl)imide
TGA	Thermogravimetric analysis
VC	Vinyl carbonate

1 Introduction

Batteries are manifested continuously in our daily lives. They have been on a long journey, emerging from a play with a frog's leg by Italian scientists and have found their way into electrical devices, *e.g.* flashlights. The first appearance of batteries in "car-like" vehicles dates back to the dawn of the first automobiles. With the advance of the chemistry, battery materials have improved the power density, capacity, cycle-life and cell-voltage of the devices and leading us to various concepts, not the least the lithium-ion battery (LIB). Today LIBs are ubiquitous in mobile phones and laptops and the research community further strives to improve the LIB to increase distance and efficiency of hybrid electric vehicles (HEVs) and fully electric vehicles (EVs) [1,2].

Conventional LIBs used in (H)EVs need a separate cooling system, keeping them at ≤ 60°C, while the power electronics are cooled to *ca.* 100°C. Thus, improving the thermal stability of LIBs to *ca.* 100°C would open for a joint cooling system, and thereby improve the overall weight and efficiency. A higher operating temperature can also make new electrode materials with improved power densities interesting, opening the path for a high-temperature LIB (HT-LIB) concept.

The electrolyte is a crucial, but often neglected, component for improving the thermal stability of batteries. Conventional LIBs contain a lithium salt, *e.g.* lithium hexafluorophosphate ($LiPF_6$), dissolved in a mixture of organic solvents, *e.g.* ethylene carbonate (EC) and dimethyl carbonate (DMC). However, these organic solvents are highly flammable and decompose at temperatures higher than 60°C, especially together with the thermally unstable $LiPF_6$ salt [3]. This decomposition is not only dangerous due to the build-up of pressure and risk of explosion, but also because of the fluorine based salts, leading to evolution of hazardous gases, *e.g.* hydrofluoric acid (HF) [3]. In recent years, one research focus has been to develop flame-retardants that can mitigate electrolyte flammability [4–6]. An alternative is to find more stable salts and solvents that improve the inherent safety of the electrolyte.

Ionic liquid (IL)-based electrolytes are promising alternatives for high-temperature applications such as the HT-LIB. ILs contain only ions and are by definition salts with melting points below 100°C, and frequently liquid at ambient temperatures. They often exhibit properties advantageous for electrolytes; low vapour pressures, high thermal stabilities, and low flammabilities [7–9], which make them suitable as HT-LIB electrolytes in combination with a Li-salt. Research on ILs has flourished the last decade [10], but no "Swiss Army Knife" IL has been found yet (and likely does not exist). It should, however, be possible to find an IL based electrolyte with all the properties needed for an HT-LIB: high thermal stability, wide electrochemical stability window, high ionic conductivity, *etc.*

In this thesis IL-based electrolytes for HT-LIBs are scrutinized for their physico-chemical properties – assessed with special emphasis on the stability, or rather **in**stability, of the materials used, including the Li-salt.

2 Batteries

Batteries are electrochemical devices that store chemical energy and transform it to electrical energy when discharged. They are classified as primary or secondary; the former being disposed after single use, while the latter can be recharged and used again. In the following the term "battery" is used synonymously for a secondary/rechargeable battery.

Today's engineers can choose from a wide variety of batteries as the power source for a diverse number of applications: electric vehicles, stationary storage, *etc*. Every battery technology has its own advantages and disadvantages, which makes them suitable for different applications. Different properties of a few selected battery concepts are listed in Table 1. The lead-acid concept is well established as a starting-lighting-ignition (SLI) battery in vehicles, because of its high power density, the wide operating temperature and its low price. Nickel-metal-hydride (NiMH) batteries are used in areas that require both high power density and high specific energy, *e.g*. cameras, power tools, and have been used in the first generations of HEVs. With similar properties, but slightly improved specific energy compared to the nickel-cadmium (NiCd) battery technology, the NiMH batteries are superior to NiCd[1]. Today, LIBs have the highest specific energies, long cycle life, and very high cell voltages, which makes them ideal for devices where low weight is a crucial factor, *e.g*. mobile phones, tablets, power tools, and (H)EVs.

Table 1: Properties of some battery technologies [11].

Chemistry	Cell voltage [V]	Spec. energy [Wh/kg]	Cycle life [#]	Power density [W/kg]	Oper. T. [°C]
Lead-acid	2.0	30	250-500	High	-40 to 60
NiCd	1.2	35	300-1000	Medium to high	-20 to 70
NiMH	1.2	90-110	500-1000	High	-20 to 65
LIB	4.0	200	1000+	Medium to high	-20 to 50

2.1 Operating Principles

The electrochemical cell is the basic unit of a battery and consists of two electrodes and an electrolyte (Figure 1). A battery is made up of one or several electrochemical cells packaged together with additional components, *e.g*. current collectors which lower the impedance of the battery and improve its electrochemical performance. The term "battery pack" is used when several batteries are connected to increase voltage or current and contain also the needed control circuitry. The battery pack in the Tesla's Model S EV is, for example, made out of thousands of small, cylindric, single-cell batteries [12].

Redox reactions take place at the electrodes when the battery is operated: oxidation at the anode and reduction at the cathode when discharged. These reactions are reversed when the cell is charged. The resulting current from the anode to cathode needs to be

[1]NiCd batteries have been banned for sale in the EU, because of the toxic cadmium, but are still used in applications where no alternatives exist.

charge-compensated by ion transport through the electrolyte. In case of liquid electrolytes, a separator is needed, to prevent the electrodes from physical contact and the battery from short-circuiting. The three basic components of the electrochemical cell are necessary for the battery to function, but usually only the electrodes store and deliver energy – why these are dubbed "active materials".

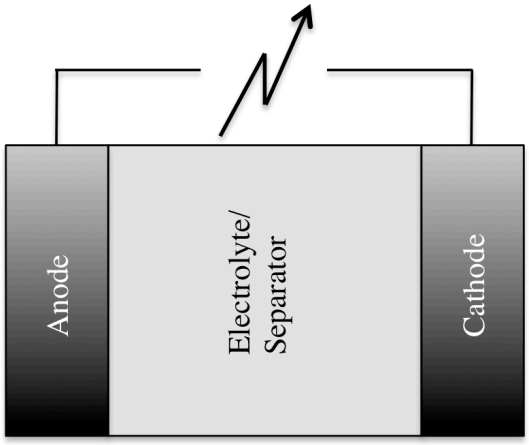

Figure 1: The three main components of an electrochemical cell.

Electrochemical cells can be interconnected in two different ways: in parallel, which improves the total capacity at fixed cell voltage, or in series, which raises the output voltage. Both configurations have their advantages and disadvantages. For a series connection the failure of a single cell leads to complete battery failure, while for a parallel connection a cell failure decreases the capacity, but the battery stays functional. In practice, a combination of parallel and series connections is most commonly used.

The most important battery properties and measures are here introduced in brief. The *output voltage* is determined by the potential difference of the half-reactions of the electrodes. LIBs have, with high cell voltages of 4 V, a large advantage over most other technologies (2 V or less, Table 1). The *specific energy* describes the amount of charge that can be extracted per kg of battery material and is highest for LIBs; approximately twice the charge can be extracted compared to a NiMH battery of the same weight, or, equivalently, half the weight can be saved for the same output charge. The *capacity* gives information about how much current or charge can be extracted over time, or how long the battery is going to work, before the active materials are depleted. The ratio between electric charge transferred during battery charge and discharge (x100%) determines the *coulombic efficiency*. The *rate capability* defines the highest current extractable from a battery. The *cycle stability* describes how the discharge capacity is reduced, *e.g.* to 80 % of its initial value, with increasing cycle number. Depending on the battery technology the cycle stability varies from 250 to more than 1000 cycles with LIBs being at the upper end of this range. However, it is notable that none of the battery technologies in Table 1 have a thermal stability higher than 70°C. This makes the HT-LIB ideal for high energy and power density, cycle and thermal stability.

2.2 The Lithium-ion Battery (LIB)

LIBs have their origin in lithium metal batteries, which made use of the low atomic weight and very negative potential of lithium enabling light-weight batteries with high output voltages of *ca*. 4.0 V. Despite the advantages of lithium as an anode material, it is for safety reasons not commonly used in its metallic form, since it can re-deposit in the form of dendrites. Therefore, higher specific capacities are neglected in favour of reliability, cycle stability, and safety leading to the LIB.

The basic principle of the LIB is that the anode and cathode are intercalation materials (Latin "intercalare" = to insert, Figure 2). During charge and discharge the electrodes expand/contract only slightly as the Li^+ are intercalated or de-intercalated [13]. The most commonly used anode materials are different kinds of graphite [14,15], where the Li^+ are intercalated between the graphene layers. The instability of aprotic electrolytes with Li^+ is rather an advantage; within the first charging cycles, lithium reacts with the electrolyte creating a solid electrolyte interphase (SEI) on the surface of the graphite anode [16]. The SEI prevents further decomposition, but still facilitates transport of the small Li^+ during charge and discharge [17]. The SEI was early stated to be thermally stable up to 120°C [18], but a detailed XPS-study later showed its decomposition close to RT [19]. The cathode materials are usually either layered, 2D-materials in terms of intercalation paths, transition-metal oxides, $LiMO_2$, with M = a combination of Co, Cr, Mn, Ni, or V [20,21], or, as price and environmental impact have been more recognized as important factors, 3D-materials like $LiMn_2O_4$ and $LiFePO_4$ have been launched as promising alternatives [22,23]. Based on the intercalation mechanism, LIBs are also called "rocking chair" batteries [24,25].

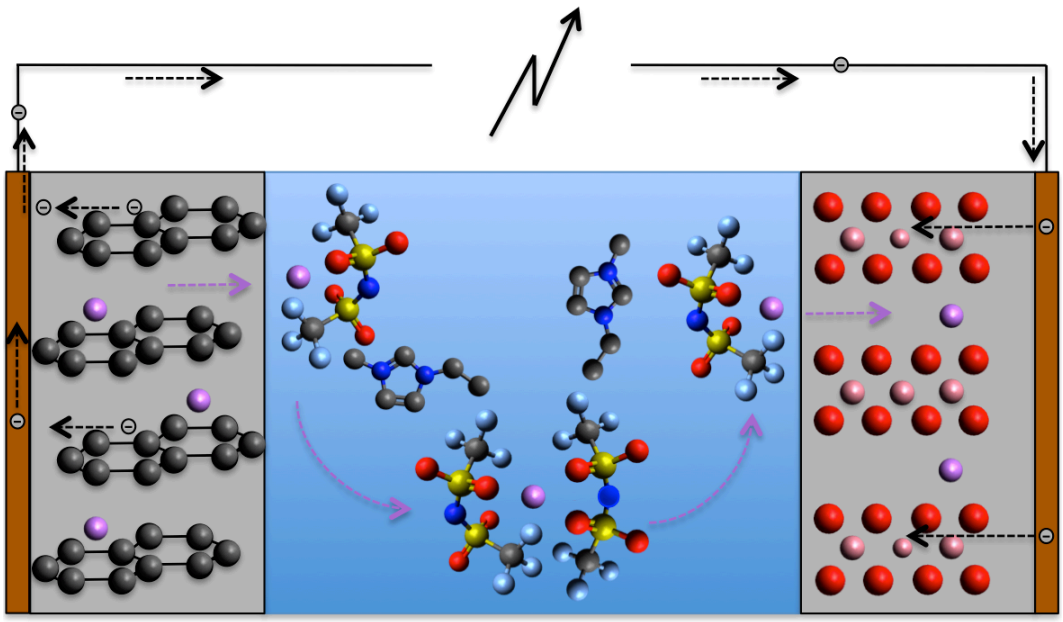

Figure 2: LIB with graphite anode, $Li_xEMI_{1-x}TFSI$ electrolyte, and $LiCoO_2$ cathode.

2.2.1 The HT-LIB

Batteries with high power densities are often used for applications with a high current demand, which is accompanied by a large heat generation. LIBs have rather high power densities and in (H)EV the current is not only high, but can also be drawn for a longer period of time. As the thermal stability of an LIB often is restricted to ≤50°C (Table 1), a separate battery cooling system is needed.

As most LIBs are not stable enough for operation at temperatures above 50-60°C [26] various measures must be taken to create working HT-LIB. The thermal stability of the electrolyte must be improved by utilising salts and solvents with higher thermal stabilities. However, increasing the thermal stability of the electrolyte is not enough, also the anode and cathode materials have to withstand the higher temperatures. The reactivity of the lithiated anode towards the electrolyte sets the upper temperature limit where chain-like decomposition reactions are irreversibly triggered [27]. The addition of an additive, *e.g.* vinyl carbonate (VC), to the electrolyte can stabilize the interphase of the anode and electrolyte and increase the thermal stability. Similar problems need to be tackled on the cathode side; the main source of heat in a battery is often the reaction between the electrolyte and the delithiated cathode [27]. A small amount of dimethylacetamide (DMAc) in the electrolyte can mitigate the reaction [28], but there is no ideal electrolyte additive to perfectly protect the electrodes at higher temperatures.

Instead of increasing the thermal stability of the electrodes used at "normal" operating temperature by modifying the electrolyte, an alternative is to use electrode materials already stable at the elevated temperatures aimed for with the HT-LIB concept. $Li_4Ti_5O_{12}$ (LTO) and chromium-rich oxidized stainless steel electrodes, $(Fe_xCr_{1-x})Cr_2O_4$ $(0.3 < x < 1)$ have been successfully tested at 60°C and 100°C, respectively [29,30]. Unfortunately, the increase in thermal stability is often accompanied by a decrease in energy density and cycle stability.

2.3 Electrolytes

An electrolyte is a medium that contains moveable ions. In the simplest form it can be a salt dissolved in a liquid solvent, *e.g.* NaCl dissolved to Na^+ and Cl^- in water. At the same time, the electrolyte has to possess many other properties (Table 2) and has to be matched with the electrode materials, current collectors and operation conditions. There are electrolytes in the form of liquids, gels, polymers, and solids. The main advantage of liquid electrolytes is their high ionic conductivity (σ).

Table 2: Important electrolyte properties.

Property	Relevance/Action
SEI formation	Protects the electrodes from degradation by reacting with the electrolyte and prevents anion intercalation.
Salt solubility	Affects the maximum possible concentration of charge carriers.
Ionic conductivity	Ensures a high mobility of charge carriers which is crucial for the power density.
Electrochemical stability window (ESW)	Determines the electrodes the electrolyte can be used with.
Wide temperature range	Increases the temperature environment the battery can be used in.
Hydrolysis stability	Improves the chemical stability and prevents HF formation.
Non-flammability	Ensures safety even in case the battery is damaged by an external hazard.
Price	Assures commercialization.

2.3.1 Conventional Electrolytes for LIBs

As mentioned above, the conventional electrolyte for LIBs is based on the $LiPF_6$ salt dissolved in a combination of different cyclic and linear carbonate organic solvents [31], *e.g.* EC and DMC. This electrolyte concept was proposed more than two decades ago by Tarascon *et al.* [32]. EC and DMC combine several important properties: EC has a high dielectric constant, that promotes lithium salt dissolution, and forms an efficient SEI layer on graphite [33]. However, the melting point, T_m, of 36°C for EC calls for usage with other solvents like DMC, which lowers both the melting point and the viscosity of the resulting electrolyte – the latter important for a high ionic conductivity. An overview of the most common organic solvents and some key properties are found in Table 3.

The classical electrolytes for LIBs have enabled thousands of charge-discharge cycles with optimized electrode configurations [26]. However, for HT-LIBs these electrolytes need to be replaced – an alternative is IL-based electrolytes [2]. Some of the fundamental physico-chemical differences between organic solvents and ILs can be seen in Table 3.

Table 3: Some important properties of common organic solvents and ILs [34–40, **I**]. The ε values are for comparable ILs.

Organic solvents	**T_m [°C]**	**$T_{b/d}$ [°C]**	**ε**	**η [mPa s]**	**FP [°C]**	**Flammable**
EC	36.4	248	89.8	1.9	160	yes
PC	-48.8	242	64.9	2.5	132	yes
DMC	4.6	91	3.1	0.6	18	yes
Ionic Liquids						
EMIFSI	-16	201	n/a	22	>300	no
EMITFSI	-18	302	12.0	40	>300	no
Pyr_{14}TFSI	-7	385	14.7	100	-	no

2.3.2 IL-based Electrolytes

ILs are by definition salts [41] which melt ≤100°C. The temperature limit is not connected to fundamental properties and is a rather arbitrary choice [42]. When the melting point is below room temperature the term "room temperature ionic liquids" (RTIL) is sometimes used – but herein we use IL for simplicity. The first known IL, ethanolammonium nitrate, was discovered in 1888 by Gabriel and Weiner [43], while the first RTIL, ethylammonium nitrate, was discovered in 1914 by Walden [44]. The number of known ILs has increased dramatically ever since, and the total number of potential ILs are estimated to be approximately one trillion (10^{18}) [10,45]. The huge number of possible cation and anion combinations, and IL properties, have given them the denomination “designer solvents” [46,47]. Indeed, the wide field of application of ILs stretches from high-temperature stable lubricants [48], over pharmaceutical ingredients [49], to energy applications [9,50], and beyond [51].

In general, ILs consist of large organic cations and inorganic anions both with a delocalized charge [8] (Figure 3). The exchange of a small anion, *e.g.* Cl^- in the IL 1-ethyl-3-methyl-imidazolium chloride (EMICl), by the tetrafluoroborate anion (BF_4^-), or the even larger bis(trifluoromethanesulfonyl)imide anion (TFSI) decreases the melting point of the corresponding ILs from 89 to 11 to -15°C, respectively [52]. An exchange of the cation results in yet bigger melting point differences [9] and altering the functional groups of the cation can change it by as much as 70°C [53]. However, the structural changes can be more delicate: shorter alkyl chains of the cation can lead to decreased viscosities and increased ionic conductivities [54].

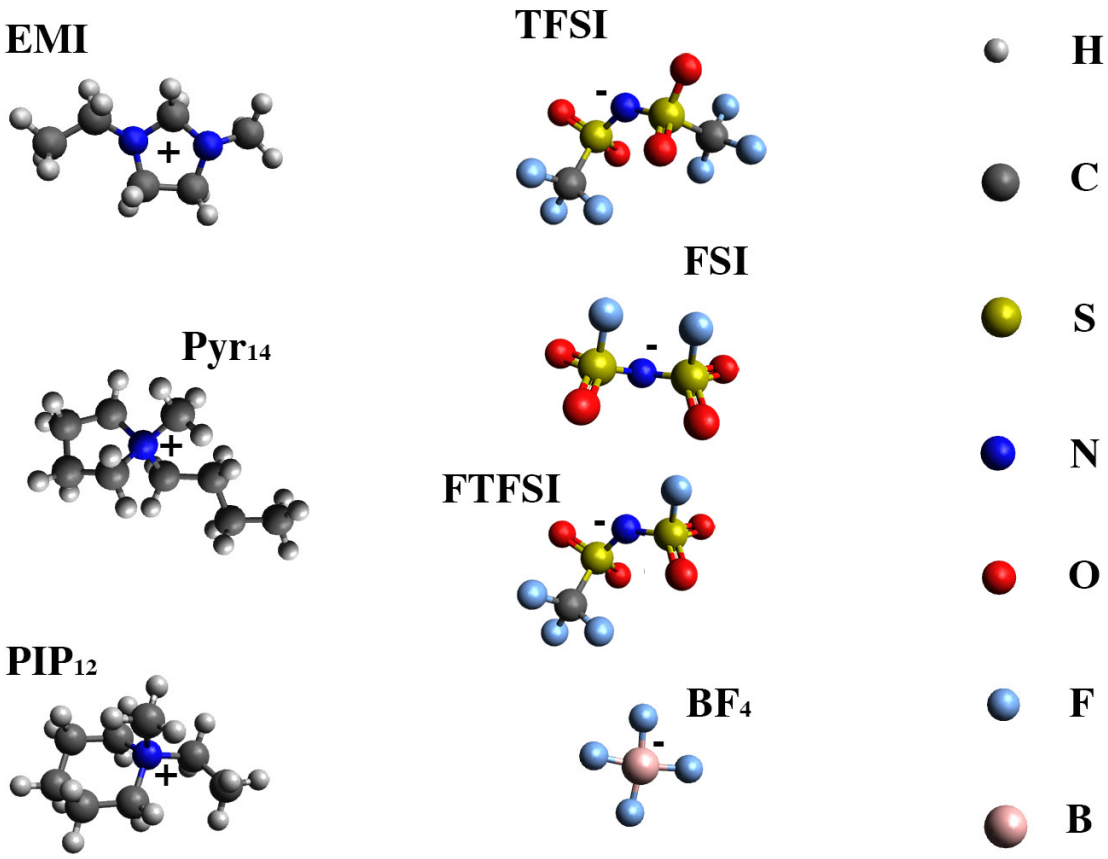

Figure 3: Structures of cations and anions of common ILs.

One of the many reasons why ILs have been considered for battery electrolytes is their high intrinsic ionic conductivities. Ionic conductivities exceeding 0.1 mS cm^{-1} at RT are often requested [55], and typically ILs have conductivities between 0.1 and 20 mS cm^{-1} [56]. However, neat ILs are not sufficient as electrolytes; a lithium salt is necessary to ensure having Li^+ transport between the electrodes. The addition of a lithium salt, however, increases the ion-ion association, and therefore also the viscosity [57]. Furthermore, association of IL ions can effectively form neutral ion-pairs that do not contribute to the ionic conductivity. The concept of ionicity describes the ratio of ions participating in conduction processes with respect of the total amount of ions present [58]. In general, the dependence of molar conductivities, Λ_m, and viscosities, η, of ILs can be described by the fractional Walden rule (1), where the exponent α corrects for differences in the activation energy of the molar conductivity and the viscosity [59].

$$\Lambda_m \, \eta^{\alpha} = const. \qquad (0 < \alpha \leq 1) \qquad (1)$$

A Walden plot, log Λ_m *vs.* η^{-1}, can be used to qualitatively describe the ionicity in ILs and IL-based electrolytes (Figure 4). The closer the ILs or electrolytes are to the reference (0.01 M $KCl_{(aq)}$) the larger the ionicity. ILs and IL-based electrolytes far below the reference line are classified as "poor ILs", those in close proximity to the line as "good ILs", and the very few found above the line are so-called "super ILs" [60]. The ion-ion association is considerable in poor IL-based electrolytes and can be a problem as the Li^+ conductivity can be restricted.

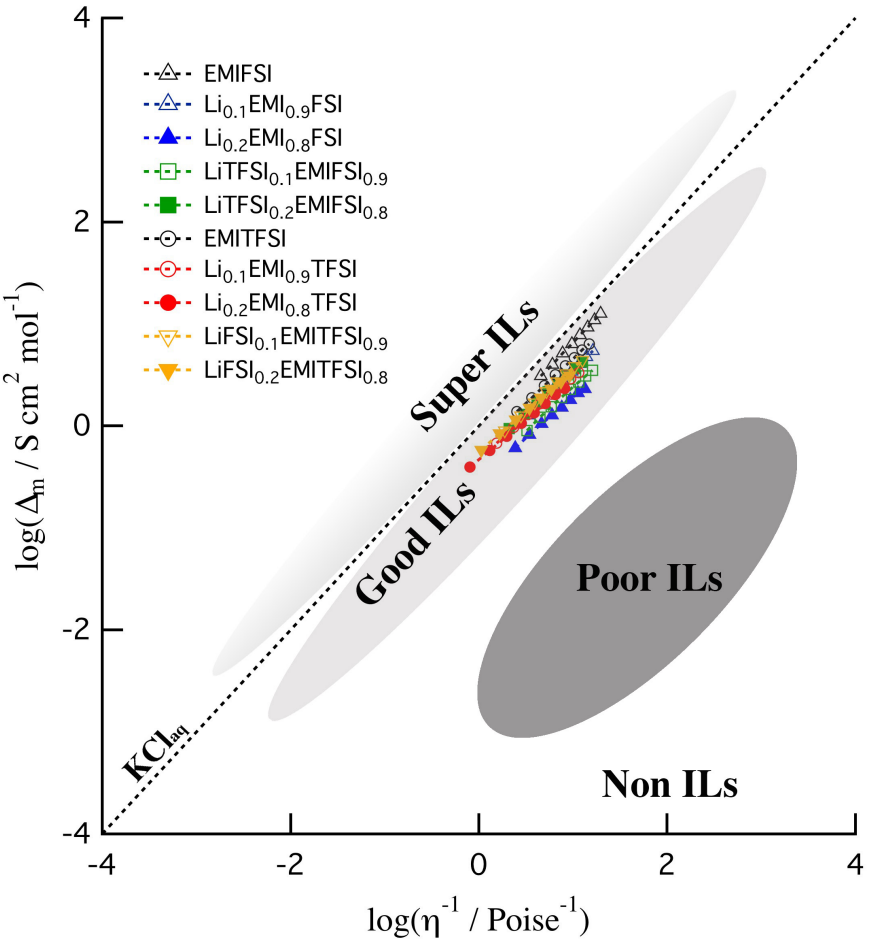

Figure 4: Walden plot with IL classification.

The Li^+ transference number, t_{Li+}, which gives the ratio of the Li^+ diffusion coefficient to the diffusion coefficient of all participating ions, should ideally approach unity [55]. The ion-ion association in "poor ILs" can lead to t_{Li+} close to 0.1 [61], due to the transport mechanism being proposed to be vehicular by *ca*. 30%, Li^+ migrates together with its solvation shell (anions), and the remainder 70% by exchange mechanisms, similar to jumping or the Grotthuss transport [62]. The implications are that bulky IL cations can have ten times higher mobilities as compared to the more associated Li^+ [63]. Solutions to mitigate this drawback have not yet been reported.

As mentioned for LIBs in general a passivation layer or an SEI is needed to ensure good cycling stability [14]. For the conventional organic solvent based electrolytes the reactions are complex between organic solvents, Li^+ and the graphite anode, but how is it for IL-based electrolytes? Yamagata *et al*. have proposed a double-layer structure being formed on the surface of different carbon electrodes in EMI bis(fluorosulfonyl)imide (EMIFSI) and EMITFSI based electrolytes [64], while Xiong *et al*. argue for the existence of a SEI on lithium electrodes in a N-butyl-N-methyl pyrrolidinium (Pyr_{14})TFSI based electrolyte [65]. Furthermore, another important question for HT-LIBs is if the existent passivation layer is stable at HT.

For battery electrolytes the most common ILs contain imidazolium (XMI) or pyrrolidinium (Pyr_{xy}) based cations [66,67] and the TFSI, FSI or BF_4^- anions [68–70]

Usually a lithium salt with the same anion as in the IL is added to the IL matrix [66,71], but a recent trend is to add a lithium salt with a different anion [67–70, **I**]. Additionally, new anions can be used *e.g.* the (fluorosulfonyl) (trifluoromethanesulfonyl)imide (FTFSI) (Figure 3), which exhibits excellent performance in electrochemical cells [76].

Despite the aforementioned problems, IL-based electrolytes have shown large promises leading to battery performance which at elevated temperatures in terms of capacity, rate capability and long-term cycle stability can be similar to or even surpass those of conventional organic electrolytes [66,75]. Recently, a phosphonium IL-based electrolyte was successfully tested in a Li/$LiCoO_2$ battery at 100°C, but the electrochemical performance, however, was rather moderate [77]. To have the same working temperature with IL-based electrolytes in HT-LIBs has not yet been reported.

2.4 Lithium Salts

The lithium salt used highly influences the overall properties of the electrolyte, why it has to be chosen carefully. In general, it must be soluble enough in the matrix to enable the concentration of charge carriers to be as large as possible. Furthermore, it needs to produce stable SEI, be non-corrosive towards electrodes and current collectors, be non-toxic, *etc*.

As mentioned above $LiPF_6$ is the most common salt for electrolytes of LIBs [27]. It can provide electrolytes with very high ionic conductivities [78], wide ESWs, and stable SEIs [79]. One drawback of this salt, however, is its auto-decomposition reaction (2) [80], which involves the release of gaseous PF_5.

$$LiPF_6\ (s) \leftrightarrow LiF(s) + PF_5(g) \qquad (2)$$

Furthermore, the salt reacts with trace water impurities to form highly toxic HF that also reacts with the SEI and the positive electrode material [81,82]. The decomposition of $LiPF_6$, which becomes more severe with increasing temperature, restricts the upper operation temperature limit of LIBs to approximately 60°C [80]. However, already at 55°C $LiPF_6$ and organic solvent based electrolytes show decreased cycle stability, which can be partly mitigated by mixing $LiPF_6$ with another lithium salt: lithium bis(oxalato)borate (LiBOB) [83].

The LiTFSI salt has been proposed as an alternative to $LiPF_6$ in order to increase the thermal stability and improve the stability against water impurities [84,85]. Indeed, LiTFSI based electrolytes have ionic conductivities comparable to those of $LiPF_6$ based [85] and have demonstrated stable operation at 60°C [86]. Improved discharge capacities, with respect to LIBs using $LiPF_6$ based electrolytes, have also been demonstrated across the temperature interval -10 to 80°C [87]. A drawback, however, is that electrolytes with LiTFSI cause corrosion of the aluminum current collector above 3.6 V [88–90], but the corrosion can be mitigated by adding a small amount of $LiPF_6$ [87], LiBOB [91], or by using very high concentrations of LiTFSI [92]. Furthermore, solvents containing a cyano-group can increase the stability against aluminum corrosion by 0.4 V [93]. In some LiTFSI IL-based electrolytes [66,94] aluminum corrosion has been prevented altogether.

The LiFSI salt is increasingly studied, because of its high thermal stability and the high ionic conductivity of its electrolytes [95–97]. The salt was reported to be stable up to 200°C and its electrolytes to exhibit higher ionic conductivities than those with $LiPF_6$ or LiTFSI [98]. The SEI formed is reported to be comparably smooth and uniform with respect to $LiPF_6$ based electrolytes [99,100]. However, there are contradictory reports about the thermal stability of LiFSI; with a possible decomposition at 75°C [101] the suitability for HT-LIBs is unclear. A more detailed discussion of the stability of LiFSI is presented in **II**.

LiBOB is another promising salt for HT-LIBs as it has a thermal stability of 300°C [102], excellent oxidation resistance up to 4.6 V *vs*. $Li^+/Li°$ [103] and forms a very stable SEI on graphite anodes [104]. The ionic conductivity is usually lower [105] or as best comparable to $LiPF_6$ based electrolytes [103]. LiBOB has a reported ability to suppress aluminum corrosion up to 5.5 V *vs*. $Li^+/Li°$ [106] and shows good high-temperature cycling capability when added to a LiTFSI in an EC and ethyl methyl carbonate (EMC) based electrolyte [91]. Its drawbacks are its sensitivity to moisture, which might lead to the production of boric acid [105] and its limited solubility in organic solvents [107].

Hundreds of lithium salts have been tested over the past decades for application in LIBs, but only less than ten have finally been established [108]. Even though the many drawbacks of $LiPF_6$ no other salt has succeeded in replacing it. For HT-LIBs no Li-salt at all has been established – yet.

3 Experimental

A detailed characterization of both the ILs themselves and the IL-based electrolytes is important, since the electrolyte has to possess many crucial properties to be viable for battery application (Table 2). In the following the main applied techniques, their purposes, and the underlying theories and methods of data analysis are introduced.

3.1 Thermal Analysis

3.1.1 Differential Scanning Calorimetry

Differential scanning calorimetry (DSC) is a common thermal characterization technique for all kinds of samples where a qualitative and/or quantitative determination of phase transitions is crucial. In ILs and for battery electrolytes in general crystallization and glass transitions can limit the application range.

The DSC is a differential method of measurement, which means that the heat flow of a sample is compared to the heat flow of a known reference and the difference is monitored [109]. Two kinds of DSC exist; "Heat Flux" and "Power Compensation" [109]. The former is used here and described in a schematic illustration of the DSC measurement chamber (Figure 5). In brief, a furnace is heated or cooled with a constant rate exposing two crucibles, one with sample and one reference, to the same heat flow. The temperature difference between the crucibles is recorded. Upon an endothermic phase transition, *e.g.* melting, the sample absorbs energy, which is observed as a sharp feature in the DSC trace (Figure 6).

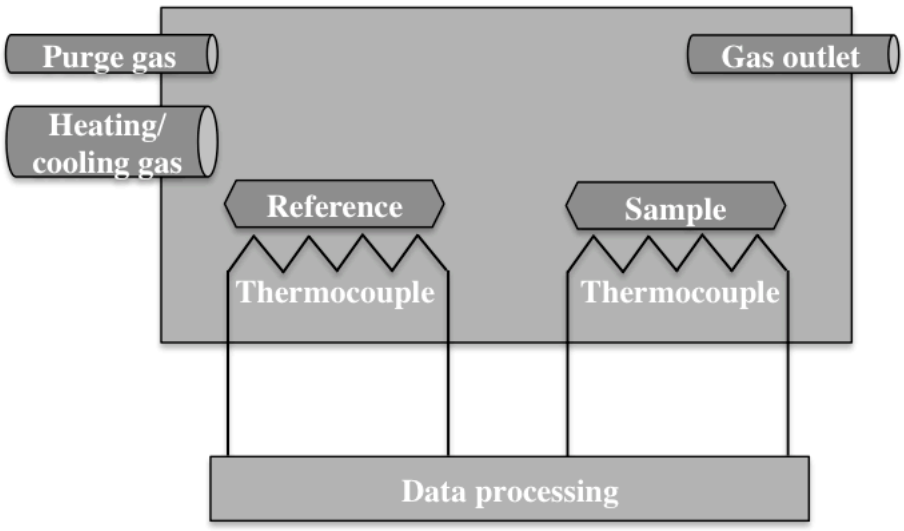

Figure 5: Schematic illustration of the DSC measurement chamber.

The DSC trace in Figure 6 is typical of an IL-based electrolyte; flat until a glass transition (glass ⇒ liquid) appears, for this particular electrolyte at *ca.* -86°C,

followed by an exothermal reaction (liquid ⇒ solid) at 38°C. At this temperature a cold crystallization takes place, whereafter the solid directly melts, visible by the endothermic peak at -22°C. To determine the features accurately, the on-set, the midpoint, and the off-set temperatures, can be used for the glass transition, while most often the peak maximum is used for defining melting and crystallization temperatures.

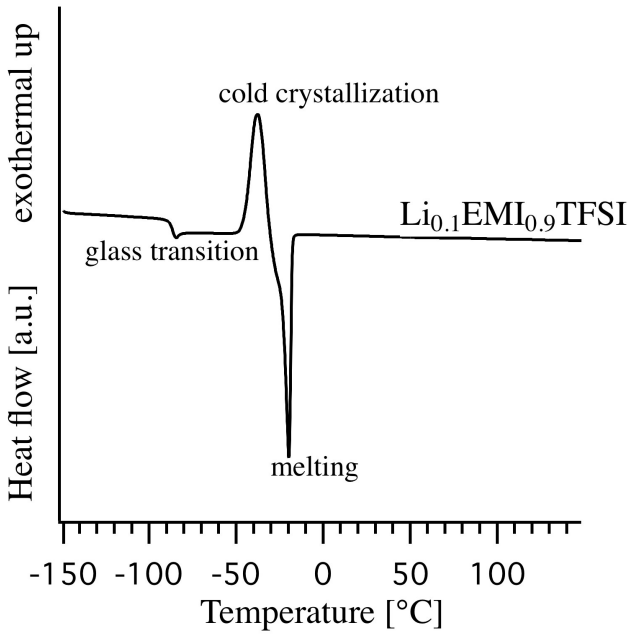

Figure 6: Typical heating trace of an IL-based electrolyte.

3.1.2 Thermogravimetric Analysis

In thermogravimetric analysis (TGA) a sample is heated according to a certain procedure, while monitoring the mass change as a function of temperature and/or time. The main components of a TGA instrument are a heating element, a temperature sensor, and a microbalance (Figure 7A). In general, TGA is performed to determine decomposition temperatures (T_d) or temperatures at which other mass loss processes, such as evaporation or sublimation, take place. Furthermore, decomposition without a change in sample mass is possible, and therefore undetectable *via* TGA, why other techniques, *e.g.* DSC, may provide the desired information. An inert purge gas (N_2 or Ar) is normally chosen to avoid sample oxidation and to not reduce the intrinsic decomposition temperature. The main functionality of the purge gas, however, is to remove reaction products, which otherwise may further react with the sample.

The choice of crucible can also affect the results – usually aluminum crucibles are favoured, because of their good thermal conductivity and their low price. For temperatures higher than 600°C, however, crucibles of alumina or platinum are to be used.

The two most often used heating procedures are *dynamic* TGA, where the heating rate is constant, and *isothermal* TGA, where the sample is kept at a constant temperature for a certain time. The T_d is mainly determined by dynamic TGA while long-term stabilities and/or adsorption processes by isothermal TGA. Both methods were applied in **I** and **II** on neat ILs, Li-salts, and electrolytes.

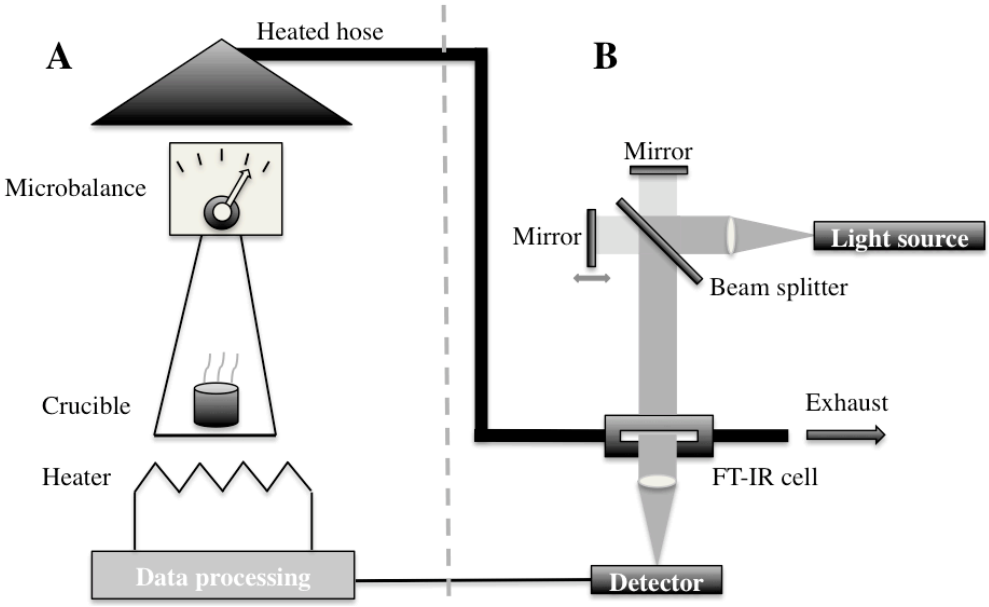

Figure 7: TGA coupled with FT-IR spectrometer.

A typical dynamic TGA heating trace displays the mass loss in % (Figure 8) as a function of temperature with process temperatures often defined by 1 or 5 % mass loss ($T_{1\%}$ and $T_{5\%}$). An alternative is the extrapolated on-set temperature (T_{onset}) by using the intersection of the extrapolated baseline of 0 % mass loss and the extrapolated tangent of the inflection point (Figure 8). T_{onset} is the temperature at which a reaction occurs spontaneously. The three temperatures are often used to determine the stabilities of samples, but to improve the reproducibility for samples without distinct decomposition processes it is recommended to use a reacted fraction (α), *e.g.* α= 0.05 % of the complete mass loss [110]. At the end of the heating curve, the off-set temperature (T_{offset}) – determined analogously to T_{onset} – can evaluate the completeness of a process (not shown). When single decomposition products might be of importance, a TGA set-up coupled to a spectrometer such as mass (MS) or Fourier transformed infrared (FT-IR) spectrometer can give additional information.

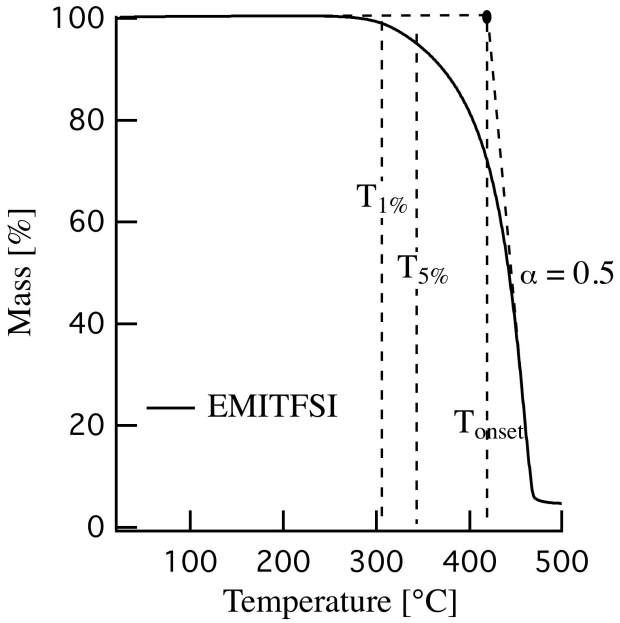

Figure 8: TGA data analysis by different methods.

The advantage of combining a FT-IR with a TGA is the possibility to identify decomposition products in real time and increase the understanding of the decomposition processes. During a TGA FT-IR measurement, the purge gas of the TGA carries the evolved decomposition products via a heated hose to the FT-IR spectrometer (Figure 7A and B), which continuously records spectra. A predefined number of these spectra are directly averaged to improve the signal to noise ratio of the resulting spectra – at the cost of decreased time-resolution. As the decomposition products are transferred from the TGA furnace to the FT-IR cell, there is also an inherent lag time of approximately one to two minutes – needed to be corrected for before correlating the FT-IR spectra features to the mass loss process(es). Vibrational spectroscopy as such is covered in chapter 3.3.

3.2 Dielectric Spectroscopy

Dielectric or impedance spectroscopy measures the frequency dependent impedance $Z^*(\omega)$ of a sample, which relates to the dielectric properties of the material. These are determined by exposing the sample to an alternating electric field and measuring its current and phase response.

The presence of an electric field generates different polarization effects in a sample; free charges are displaced in and against the direction of the electric field (atomic or ionic polarization), while dipoles orient themselves with the positive and negative pole in respective direction (dipolar polarization). For alternating electric fields, the response of the material is dependent on the applied frequency: both of the mentioned effects are present at low frequencies, while the orientational polarization disappears as a result of inertia when the frequency is increased to approximately 10^{10} Hz. At 10^{13} Hz the alternating electric field switches too fast for the atomic polarization to

react, and finally at 10^{16} Hz not even the electronic polarization, where the electron cloud shifts with respect to the atomic core, is displaced anymore [111] (Figure 9). Thus, different effects can be targeted as a function of frequency; for IL-based battery electrolytes the ionic conductivity is the property of interest where all ions participate: Li^+, the IL cation, the IL anion and the anion of the lithium salt. Furthermore, Li^+ can be coordinated to the anions and migrate as part of different complexes, why the main part of the conductivity does not necessarily arise from these species [112].

A schematic of the cell used (Figure 10) shows: two electrodes placed in a brass casing, where Teflon© acts as an insulator and defines the volume of the sample. The physics behind this technique is that an oscillating potential difference between two electrodes (eq. 3), with ω as the angular frequency $\omega = 2\pi f$, leads to an alternating direction of the electric field. The resulting polarization effects can be measured as the alternating current response (eq. 4). The phase difference, ϕ between the applied voltage and the measured current is due to the time needed for polarization effects to get oriented.

$$U^*(t) = U_0 \exp(i\omega t) \quad (3)$$

$$I^*(t) = I_0 \exp(i\omega t + \varphi) \quad (4)$$

The ratio between the complex parts of the applied voltage and measured current (eq. 5) gives the impedance Z*(ω), from which the permittivity of the electrolyte, $\varepsilon(\omega)$, (eq. 6) and σ(ω) (eq. 7) are extracted. In this work, frequencies between 10^{-1} and 10^7 Hz were routinely applied to extract the ionic conductivity.

$$Z^*(\omega) = \frac{U^*(\omega)}{I^*(\omega)} \quad (5)$$

$$\varepsilon(\omega) = \frac{1}{i\omega C_0 Z(\omega)} \quad ;(C_0, \textit{ empty cell capacity}) \quad (6)$$

$$\sigma(\omega) = i\omega\varepsilon_0\varepsilon(\omega) \quad ;(\varepsilon_0, \textit{ vacuum permittivity}) \quad (7)$$

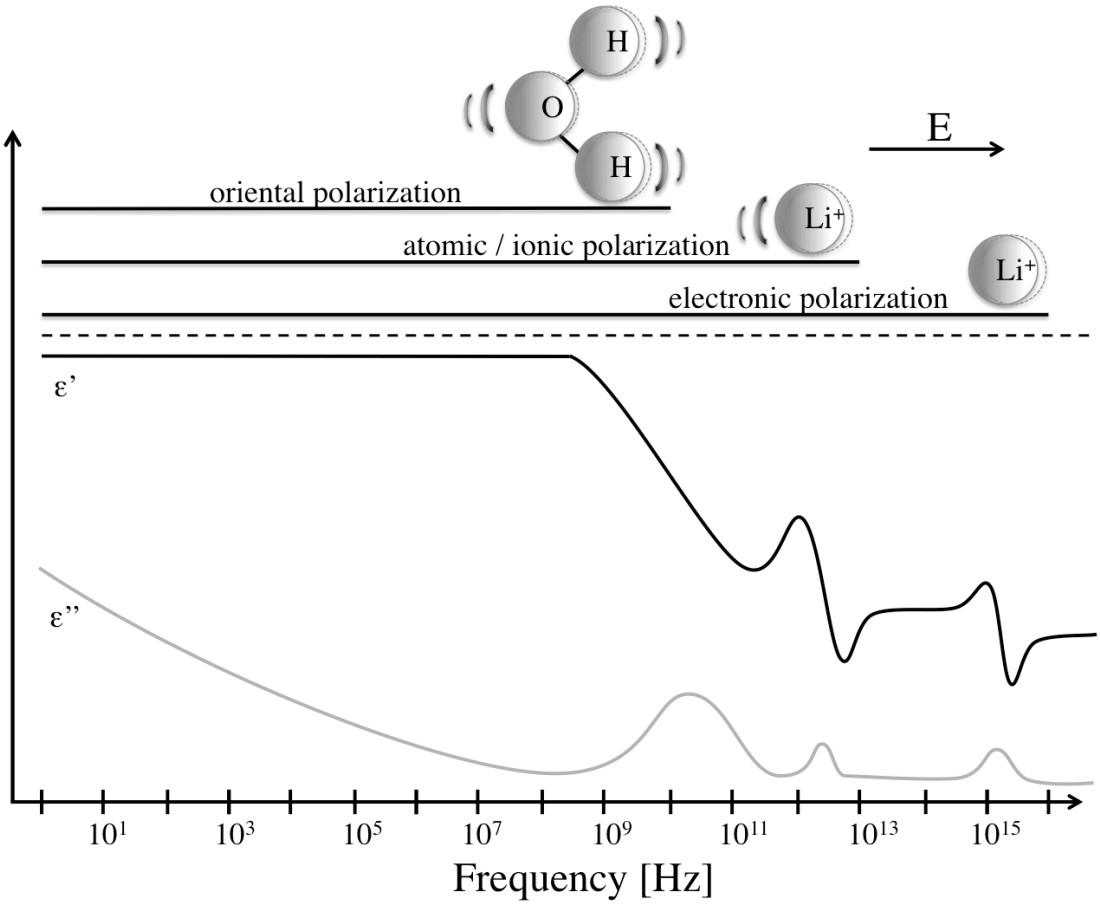

Figure 9: Response of a dielectric sample to an electric field.

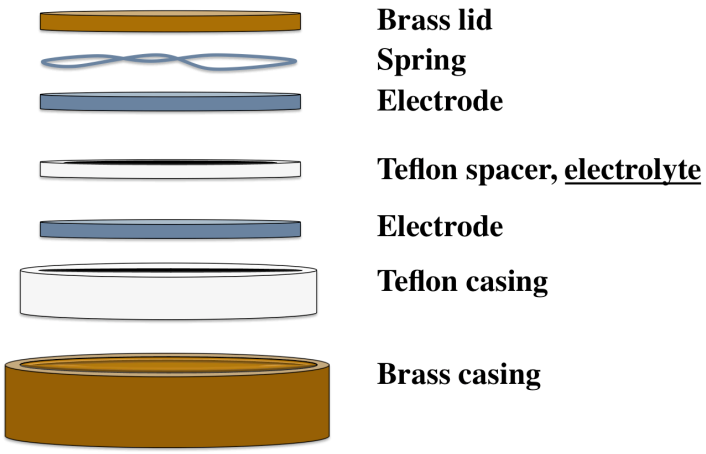

Figure 10: Dielectric spectroscopy measurement cell set-up.

3.3 Vibrational Spectroscopy

Vibrational spectroscopy comprises the interaction of electromagnetic waves with matter. Depending on the molecules, their symmetry and the atoms involved, only certain frequencies of electromagnetic waves induce vibrational modes. Every molecule consists of a certain number of atoms, which determine the degree of freedom of the molecule. In Cartesian coordinates, every atom (N) in the molecule can move in three directions, but there are three combinations that describe the movement of the whole molecule (translations) and additionally three where it rotates as a whole (rotations), which leaves a total of 3N-6 vibrational degrees of freedom. For a linear molecule two of the rotations are identical, which results in 3N-5 vibrations. All vibrations contain changes of interatomic lengths and/or angles with characteristic frequencies. Classically, a simple spring model can be used to visualize the factors determining the different frequencies [113]: an atom is bound to a large mass by a weightless spring with a characteristic force constant, *f*. To move the atom a distance *x* out of its equilibrium position x_0, a force *F* has to be applied. This force is in opposite direction to the force holding the atom in its position. The resulting equation is known as Hooke's law (eq. 8).

$$F = -fx \tag{8}$$

Newton's second law describes the relation of force, mass, and acceleration:

$$F = m\frac{dx^2}{dt^2} \tag{9}$$

Equating these two formulas gives:

$$m\frac{dx^2}{dt^2} = -fx \tag{10}$$

The following equation is the solution to (eq. 10) and describes a harmonic oscillator:

$$x = x_0 \cos(2\pi\nu t + \varphi) \tag{11}$$

Combining the equations above and solving for the frequency ν gives:

$$\nu = \frac{1}{2\pi}\sqrt{\frac{f}{m}} \tag{12}$$

Equation (12) determines the frequency with which a mass is vibrating when connected to a very large mass by an elastic spring. Thus the force constant (*i.e.* bond strength) and the mass (atom number incl. isotope) determine the vibration frequency – the stronger the atoms are attracted to each other and the lighter they are the higher the vibration frequency.

3.3.1 IR Spectroscopy

Infrared (IR) spectroscopy uses mid- and far-infrared light with wavelengths from 2.5 to 1000 μm to analyse materials [113]. A sample is exposed to a continuous infrared spectrum with the intensity I_0. Depending on the bonds and atoms and the concentration, vibrational states are excited by photons (Figure 11). These photons are absorbed by the material and lead to absorption bands in the resulting spectrum. In an IR spectrum the transmittance, T, spectrum is provided (I/I_0) (eq. 13) as a function of wavenumber $\bar{\nu}$, where the wavenumber is the inverse wavelength.

$$T = \frac{I(\bar{\nu})}{I_0(\bar{\nu})} \tag{13}$$

The absorption, A, is proportional to the sample thickness or light path of the laser beam, l, the molar absorptivity, ε, and the concentration of the absorbing species, c (eq. 14). This makes IR spectroscopy not only a qualitative, but also a quantitative tool.

$$A = l\,\varepsilon\,c \tag{14}$$

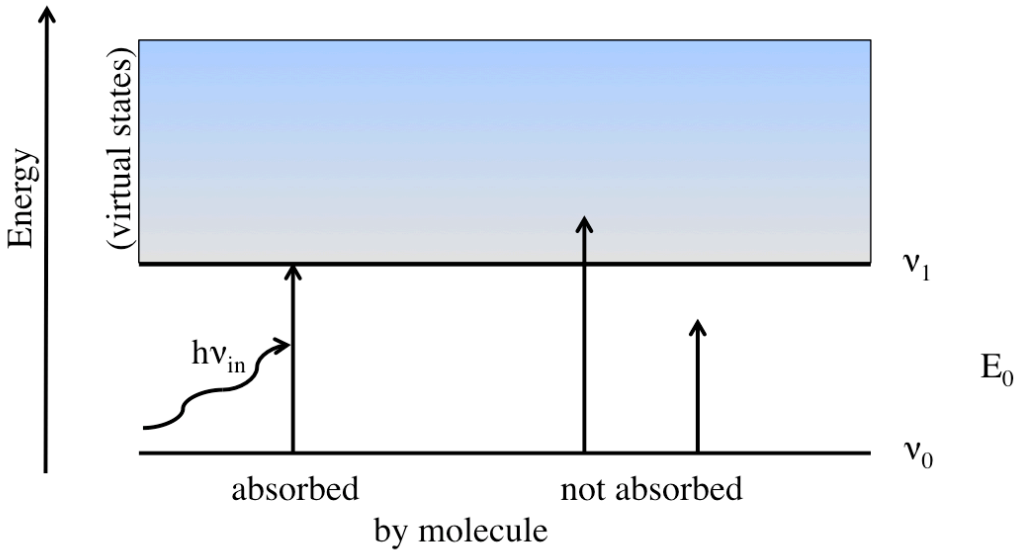

Figure 11: Absorption of photons by the transition of vibrational states.

For a vibration to be IR active it must change the molecular dipole moment, μ, why diatomic molecules like O_2 and N_2 are not detectable by IR spectroscopy.

3.3.2 Raman Spectroscopy

The Raman effect is due to the change of energy of a photon when a monochromatic laser beam irradiates matter [114]. A vibrational state is temporarily raised to a "virtual state", energetically situated between the highest vibrational and the next highest electronic state. This transition is not quantized and the resulting emitted photon has either a lower energy (Stokes scattering), higher energy (anti-Stokes scattering) or the same energy (Rayleigh scattering) as the incident photon (Figure 12). At room temperature, the molecule is usually in its ground state and hence its vibrations (ν_0). Accordingly, the probability of detecting Stokes transitions are higher than anti-Stokes – resulting in higher intensities and a better signal to noise ratio why usually only the Stokes part of the Raman spectra is considered.

As for IR, Raman spectroscopy is qualitative and quantitative as the intensities of vibrations are proportional to the density of scattering molecules. An example of a section of a Raman spectrum together with its fitted bands and their vibrational origins are shown in Figure 13. The same molecule can give rise to a band at a shifted wavenumber when in a different local surrounding, as *e.g.* bond strengths can be changed.

For a vibration to be Raman active it must change the polarisability of the molecule, why homo diatomic molecules are Raman active and detectable (in contrast to IR). As a rule of thumb, symmetric molecules are Raman active, while asymmetric molecules are IR active, why Raman and IR spectroscopy often are considered as highly complementary methods.

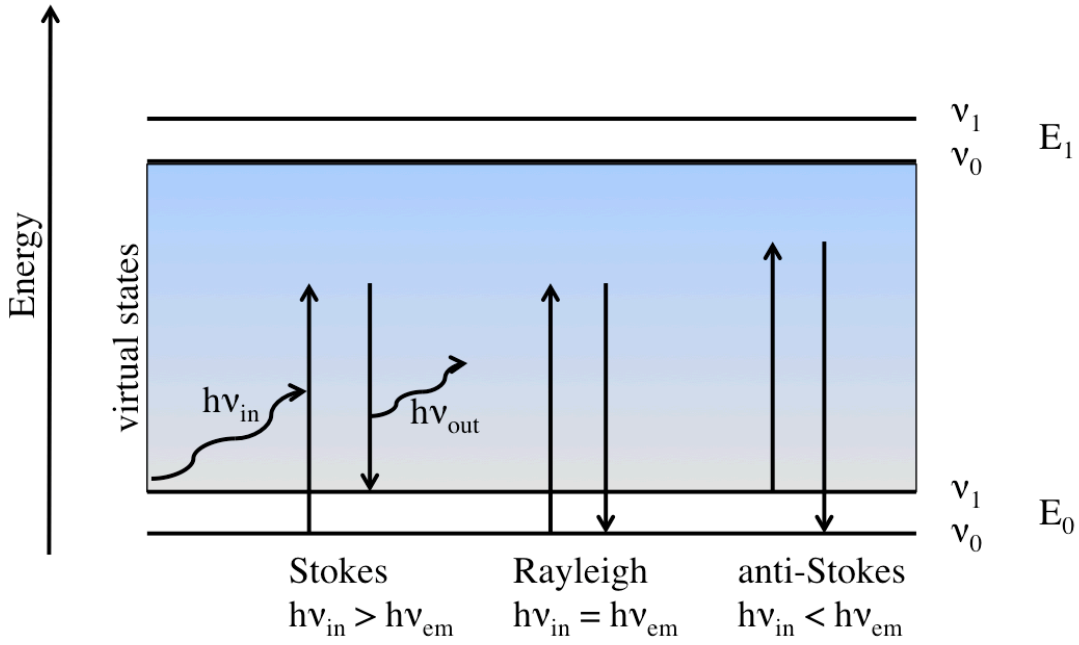

Figure 12: Vibrational transitions during spectroscopic measurements.

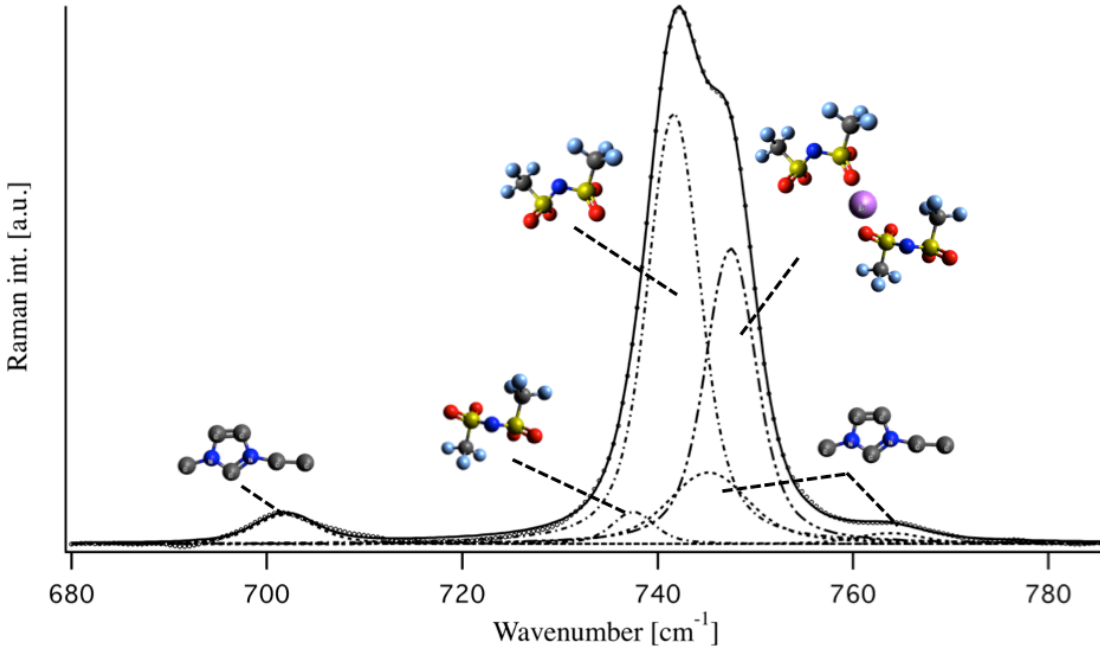

Figure 13: Raman spectrum of $Li_{0.2}EMI_{0.8}TFSI$ with band assignments.

3.4 Linear Sweep Voltammetry

Linear sweep voltammetry (LSV) is used to determine the ESW of the electrolyte – an important property that gives a first hint of viable electrolyte-electrode combinations and working ranges. Experimentally, a separator is soaked with electrolyte and placed between two electrodes, usually in a “coin” or "Swagelok" type electrochemical cell (Figure 14A). For characterizing LIB electrolytes, lithium is most often used as reference and counter electrode, while the working electrode is usually made of stainless steel, platinum, or gold. Starting from the open circuit voltage (OCV), where no net current flows, the potential *vs*. $Li^+/Li°$ is increased at a constant sweep rate, *e.g*. 0.5 mV/s. The measured current increases with the appearance of oxidative processes. Often, a cut-off current density of 0.1 mA cm^{-2} is used to determine the starting point of electrolyte degradation. Separate runs using separate cells are made for the oxidative stability and the reductive stability. A typical LSV curve of one of the electrolytes from **I** is shown in Figure 14B, with an ESW of *ca*. 5 V.

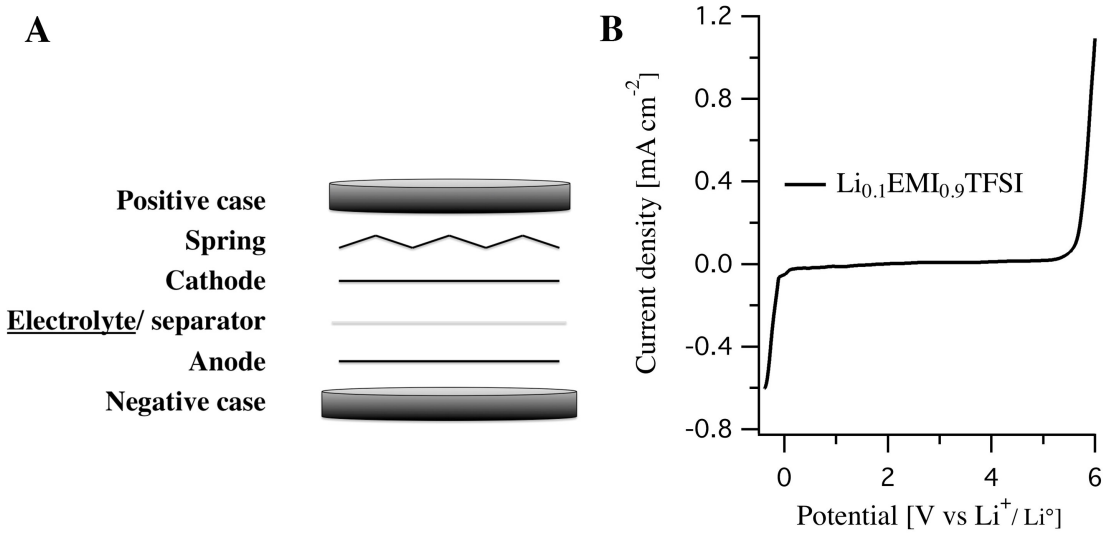

Figure 14: Electrochemical test cell and a typical voltammogram.

4 Summary of Appended Papers

4.1 Paper I

In this paper we investigated the fundamental properties of IL based electrolytes for high-temperature application. All of the analysed electrolytes had wide liquid ranges and were thermally stable above 160°C and even exhibited long-term stabilities over 10 hours at 100°C (Figure 15). The ionic conductivities were acceptable at RT and further increased with temperature; showing excellent ionic conductivities at 90°C. The $LiTFSI_{0.2}EMIFSI_{0.8}$ electrolyte where two anions are present was especially promising, as in terms of thermal stability and ionic conductivity it outperformed the other electrolytes. The electrochemical stability window was ≥ 4 V and in general increased with TFSI content (Figure 15).

A detailed Raman analysis showed Li^+ solvation numbers of *ca*. 2 for all the electrolytes, where the FSI based were somewhat larger. No distinct anion coordination preference for Li^+ was to be concluded, as the data were ambiguous. Possibly $LiTFSI_{0.2}EMIFSI_{0.8}$ indicates a synergetic effect of mixed anion IL based electrolytes.

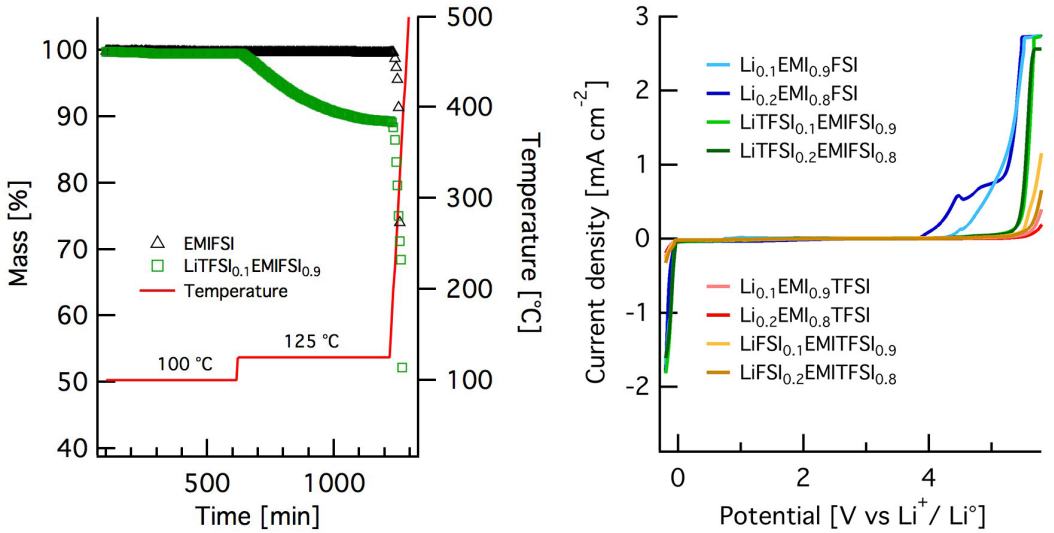

Figure 15: Thermal stability of an IL, an electrolyte, and ESWs of all electrolytes.

4.2 Paper II

Here we compared three commercial LiFSI salts in terms of their thermal stabilities and phase transitions. Additionally, we performed a combined Raman and IR vibrational spectroscopy analysis to if possible find any molecular level differences. Indeed, Raman spectroscopy uncovered an impurity ($LiClO_4$) in one of the salts, which from the literature can be expected to be a left-over from the synthesis process. The impurity was likely also the cause for an additional decomposition feature observed in the TGA measurements (Figure 16). The results illustrate the importance of always assuring a high and uniform quality of the LiFSI salt used for battery electrolyte application.

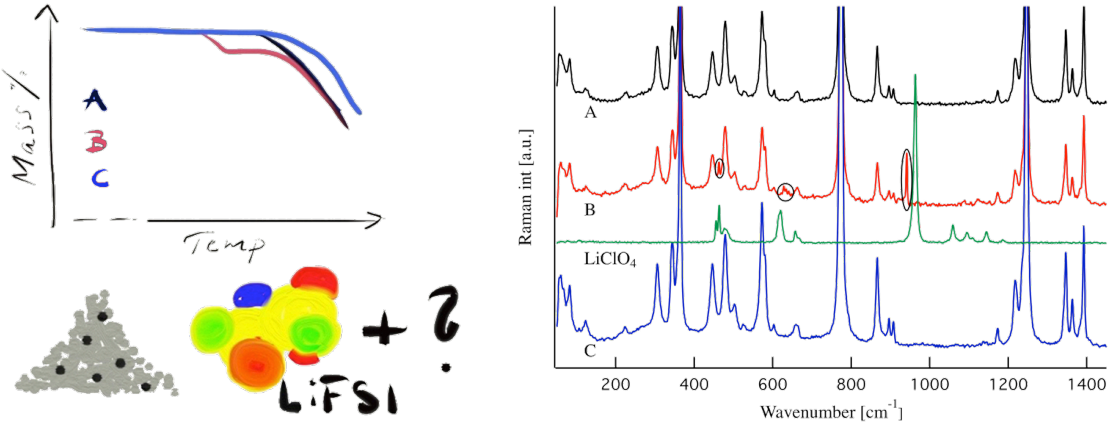

Figure 16: Dynamic TGA results and Raman spectra of three LiFSI salts.

5 Conclusions and Outlook

- IL based electrolytes are a viable path for HT-LIB operating at *ca*. 100°C.

- A synergetic effect of having both TFSI and FSI anions present in the electrolyte exists for a certain ratio. This results in increased thermal stabilities and high ionic conductivities. Possibly a mixed FSI and TFSI solvation of Li^+ exists in such electrolytes.

- The quality of the LiFSI salt is highly dependent on the supplier/manufacturer and possibly originates in the synthesis process. Amongst other factors, impurities present alter the thermal stabilities of the salts.

- Even though the IL-based electrolytes showed promising properties at a high temperature, their final viability as HT-LIB electrolytes has to be tested by cycling experiments, *etc*.

- Transport numbers should if possible be determined for the mixed systems to increase the understanding of these electrolytes.

- A further tailoring of properties can and should be applied by the application of additives, *e.g*. high-temperature stable organic or silicon based solvents, to further increase the thermal stability, ionic conductivity and/or other properties.

Acknowledgements

First of all, I would like to express my deepest gratitude to my supervisors Patrik and Johan for their continuous and excellent support, their patience, their guidance and for the inspiring and motivating discussions we have had. Also, I want to thank Patrik for giving me the opportunity to do a PhD in such an interesting field.

Even though there are a lot of high quality devices at KMF, some of them seem not to be of continuous high quality. For all his time, helping out, and solving problems I would like to thank Ezio.

Everyone at KMF and beyond, thanks for providing a scientific environment, where ideas can be discussed to increase the understanding in all matters. Especially, I would like to thank Luis for the discussions about Raman spectroscopy and the fitting procedure and Andrea for the scientific discussions and sharing all "components" of teaching duties.

All of us need to start at some point and even though this has been before quite some time, now, I would like to thank two KMF alumni members for introducing me into different measurement techniques: Maciej & Jagath, thanks.

Scientific life is interesting in so many ways, however, it can only be completely fulfilling when there is also some time to relax. Therefore, I would like to thank my family and friends for *cough* "recharging my batteries", their support and encouragements.

Thanks to all of you!

Yours truly,
Manfred

Gothenburg, the 30th of October 2015

References

[1] J.B. Goodenough et al., The Li-ion rechargeable battery: A perspective, J. Am. Chem. Soc. 135 (2013) 1167–76. doi:10.1021/ja3091438.

[2] B. Scrosati et al., Lithium batteries: Status, prospects and future, J. Power Sources 195 (2010) 2419–2430. doi:10.1016/j.jpowsour.2009.11.048.

[3] S.F. Lux et al., The mechanism of HF formation in $LiPF_6$ based organic carbonate electrolytes, Electrochem. Commun. 14 (2012) 47–50. doi:10.1016/j.elecom.2011.10.026.

[4] X. Wang et al., Nonflammable Trimethyl Phosphate Solvent-Containing Electrolytes for Lithium-Ion Batteries: I. Fundamental Properties, J. Electrochem. Soc. 148 (2001) A1058. doi:10.1149/1.1397773.

[5] H. Ota et al., Effect of cyclic phosphate additive in non-flammable electrolyte, J. Power Sources 119-121 (2003) 393–398. doi:10.1016/S0378-7753(03)00259-3.

[6] H. Nakagawa et al., Application of nonflammable electrolyte with room temperature ionic liquids (RTILs) for lithium-ion cells, J. Power Sources 174 (2007) 1021–1026. doi:10.1016/j.jpowsour.2007.06.133.

[7] S. Aparicio et al., Thermophysical Properties of Pure Ionic Liquids: Review of Present Situation, Ind. Eng. Chem. Res. 49 (2010) 9580–9595. doi:10.1021/ie101441s.

[8] M. Armand et al., Ionic-liquid materials for the electrochemical challenges of the future, Nat. Mater. 8 (2009) 621–9. doi:10.1038/nmat2448.

[9] A. Matic et al., Ionic liquids for energy applications, MRS Bull. 38 (2013) 533–537. doi:10.1557/mrs.2013.154.

[10] F. Endres et al., Air and water stable ionic liquids in physical chemistry, Phys. Chem. Chem. Phys. 8 (2006) 2101–16. doi:10.1039/b600519p.

[11] T.B. Reddy, Linden's Handbook of Batteries, Fourth Ed., McGraw-Hill Education, 2011.

[12] P. Stenquist, Tesla Model S Offers a Lesson in Electric-Vehicle Economics, New York Times. (2012). http://wheels.blogs.nytimes.com/2012/06/25/tesla-model-s-offers-a-lesson-in-electric-vehicle-economics/?_r=0 (accessed October 6, 2015).

[13] T. Ohzuku, Formation of Lithium-Graphite Intercalation Compounds in Nonaqueous Electrolytes and Their Application as a Negative Electrode for a Lithium Ion (Shuttlecock) Cell, J. Electrochem. Soc. 140 (1993) 2490. doi:10.1149/1.2220849.

[14] S. Megahed et al., Lithium-ion rechargeable batteries, J. Power Sources 51 (1994) 79–104. doi:10.1016/0378-7753(94)01956-8.

[15] K. Sawai et al., Carbon materials for lithium-ion (shuttlecock) cells, Solid State Ionics 69 (1994) 273–283. doi:10.1016/0167-2738(94)90416-2.

[16] S.-K. Jeong et al., Surface Film Formation on Graphite Negative Electrode in Lithium-Ion Batteries: AFM Study in an Ethylene Carbonate-Based Solution, J. Electrochem. Soc. 148 (2001) A989. doi:10.1149/1.1387981.

[17] E. Peled, The Electrochemical Behavior of Alkali and Alkaline Earth Metals in Nonaqueous Battery Systems—The Solid Electrolyte Interphase Model, J. Electrochem. Soc. 126 (1979) 2047. doi:10.1149/1.2128859.

[18] A. Du Pasquier, Differential Scanning Calorimetry Study of the Reactivity of Carbon Anodes in Plastic Li-Ion Batteries, J. Electrochem. Soc. 145 (1998) 472. doi:10.1149/1.1838287.

[19] A.M. Andersson et al., Chemical Composition and Morphology of the Elevated Temperature SEI on Graphite, J. Electrochem. Soc. 148 (2001) A1100. doi:10.1149/1.1397771.

[20] T. Ohzuku et al., Why transition metal (di) oxides are the most attractive materials for batteries, Solid State Ionics 69 (1994) 201–211. doi:10.1016/0167-2738(94)90410-3.

[21] M.M. Thackeray, Lithiated Oxides for Lithium Ion Batteries, J. Electrochem. Soc. 142 (1995) 2558–2563.

[22] M.K. Aydinol et al., First-Principles Prediction of Insertion Potentials in Li-Mn Oxides for Secondary Li Batteries, J. Electrochem. Soc. 144 (1997) 3832. doi:10.1149/1.1838099.

[23] A.K. Padhi et al., Effect of Structure on the Fe3/Fe2 Redox Couple in Iron Phosphates, Electrochem. Soc. 144 (1997) 1609–1613.

[24] B. Scrosati, Lithium Rocking Chair Batteries: An Old Concept?, J. Electrochem. Soc. 139 (1992) 2776–2781.

[25] T. Ohzuku et al., Innovative insertion material of $LiAl_{1/4}Ni_{3/4}O_2$ ($R\bar{3}m$) for lithium-ion (shuttlecock) batteries, J. Power Sources 68 (1997) 131–134. doi:10.1016/S0378-7753(97)02516-0.

[26] B. Diouf et al., Potential of lithium-ion batteries in renewable energy, Renew. Energy 76 (2015) 375–380. doi:10.1016/j.renene.2014.11.058.

[27] K. Xu, Electrolytes and interphases in li-ion batteries and beyond., Chem. Rev. 114 (2014) 11503–618. doi:10.1021/cr500003w.

[28] W. Li et al., Inhibition of solid electrolyte interface formation on cathode particles for lithium-ion batteries, J. Power Sources 168 (2007) 258–264. doi:10.1016/j.jpowsour.2007.02.055.

[29] J. Guo et al., A novel $Li_4Ti_5O_{12}$-based high-performance lithium-ion electrode at elevated temperature, J. Mater. Chem. A. 3 (2015) 4938–4944. doi:10.1039/C4TA05660D.

[30] F. Mestre-Aizpurua et al., High temperature lithium cells using conversion oxide electrodes, J. Appl. Electrochem. 40 (2010) 1365–1370. doi:10.1007/s10800-010-0103-0.

[31] G.E. Blomgren, Electrolytes for advanced batteries, J. Power Sources 81-82 (1999) 112–118. doi:10.1016/S0378-7753(99)00188-3.

[32] J. Tarascon et al., New electrolyte compositions stable over the 0 to 5 V voltage range and compatible with the $Li_{1+x}Mn_2O_4$/carbon Li-ion cells, Solid State Ionics 69 (1994) 293–305. doi:10.1016/0167-2738(94)90418-9.

[33] J.M. Tarascon et al., Issues and challenges facing rechargeable lithium batteries, Nature 414 (2001) 359–367.

[34] R.-S. Kühnel et al., Mixtures of ionic liquid and organic carbonate as electrolyte with improved safety and performance for rechargeable lithium batteries, Electrochim. Acta 56 (2011) 4092–4099. doi:10.1016/j.electacta.2011.01.116.

[35] D.M. Fox et al., Flammability and Thermal Analysis Characterization of Imidazolium-Based Ionic Liquids, Ind. Eng. Chem. Res. 47 (2008) 6327–6332. doi:10.1021/ie800665u.

[36] CoorsTek, CoorsTek, (n.d.). https://coorstekchem.com/sites/default/files/IolyteP2-DataSheet.pdf (accessed November 3, 2015).

[37] CoorsTek, CoorsTek, (n.d.). https://coorstekchem.com/sites/default/files/IolyteP1-EMIM_TFSI_DataSheet.pdf (accessed November 3, 2015).

[38] H. Weingärtner, The static dielectric permittivity of ionic liquids, J. Mol. Liq. 192 (2014) 185–190. doi:10.1016/j.molliq.2013.07.020.

[39] M. Montanino et al., Physical and electrochemical properties of binary ionic liquid mixtures: (1−x) PYR_{14}TFSI–(x) $PYR_{14}IM_{14}$, Electrochim. Acta 60 (2012) 163–169. doi:10.1016/j.electacta.2011.11.030.

[40] M. Nádherná et al., Lithium bis(fluorosulfonyl)imide–PYR_{14}TFSI ionic liquid electrolyte compatible with graphite, J. Power Sources 196 (2011) 7700–7706. doi:10.1016/j.jpowsour.2011.04.033.

[41] K.E. Johnson, What's an Ionic Liquid?, Electrochem. Soc. (2007) 38–41.

[42] K. Seddon, Ionic liquids: A taste of the future, Nat. Mater. 6 (2003) 363–366.

[43] S. Gabriel et al., Ueber einige Abkömmlinge des Propylamins, Berichte Der Dtsch. Chem. Gesellschaft. 21 (1888) 2669–2679. doi:10.1002/cber.18880210288.

[44] P. Walden, Ueber die Molekulargrösse und elektrische Leitfähigkeit einiger geschmolzenen Salze, Bull. Acad. Imper. Sci. 1 (1914) 405–422.

[45] J.D. Holbrey et al., Ionic Liquids, Clean Technol. Environ. Policy 1 (1999) 223–236. doi:10.1007/s100980050036.

[46] K.R. Seddon, Ionic Liquids for Clean Technology, J. Chem. Technol. Biotechnol. 68 (1997) 351–356.

[47] M.J. Earle et al., Ionic liquids. Green solvents for the future, Pure Appl. Chem. 72 (2000) 1391–1398. doi:10.1351/pac200072071391.

[48] V. Pejaković et al., Influence of temperature on tribological behaviour of ionic liquids as lubricants and lubricant additives, Lubr. Sci. 26 (2014) 107–115. doi:10.1002/ls.1233.

[49] P.M. Dean et al., Exploring an anti-crystal engineering approach to the preparation of pharmaceutically active ionic liquids, Cryst. Growth Des. 9 (2009) 1137–1145. doi:10.1021/cg8009496.

[50] W. Kubo et al., Quasi-solid-state dye-sensitized solar cells using room temperature molten salts and a low molecular weight gelator, Chem. Commun. (Camb). (2002) 374–375. doi:10.1039/b110019j.

[51] Q. Zhang et al., Recent advances in ionic liquid catalysis, Green Chem. 13 (2011) 2619. doi:10.1039/c1gc15334j.

[52] H.L. Ngo et al., Thermal properties of imidazolium ionic liquids, Thermochim. Acta 357-358 (2000) 97–102. doi:10.1016/S0040-6031(00)00373-7.

[53] B. Baek et al., Pyrrolidinium cation-based ionic liquids with different functional groups: Butyl, butyronitrile, pentenyl, and methyl butyrate, Int. J. Electrochem. Sci. 6 (2011) 6220–6234.

[54] K. Kim et al., Effect of alkyl-chain length of imidazolium based ionic liquid on ion conducting and interfacial properties of organic electrolytes, J. Ind. Eng. Chem. 26 (2015) 136–142. doi:10.1016/j.jiec.2014.11.025.

[55] J.B. Goodenough et al., Challenges for Rechargeable Li Batteries, Chem. Mater. 22 (2010) 587–603. doi:10.1021/cm901452z.

[56] A. Lewandowski et al., Ionic liquids as electrolytes for Li-ion batteries—An

overview of electrochemical studies, J. Power Sources 194 (2009) 601–609. doi:10.1016/j.jpowsour.2009.06.089.

[57] S. Tsuzuki et al., Origin of the low-viscosity of [emim][$(FSO_2)_2N$] ionic liquid and its lithium salt mixture: Experimental and theoretical study of self-diffusion coefficients, conductivities, and intermolecular interactions, J. Phys. Chem. B. 114 (2010) 16329–16336. doi:10.1021/jp106870v.

[58] D.R. MacFarlane et al., On the concept of ionicity in ionic liquids, Phys. Chem. Chem. Phys. 11 (2009) 4962–7. doi:10.1039/b900201d.

[59] C. Austen Angell et al., Ionic Liquids: Past, present and future, Faraday Discuss. 154 (2012) 9. doi:10.1039/c1fd00112d.

[60] C.A. Angell et al., Parallel developments in aprotic and protic ionic liquids: Physical chemistry and applications, Acc. Chem. Res. 40 (2007) 1228–1236. doi:10.1021/ar7001842.

[61] T. Frömling et al., Enhanced lithium transference numbers in ionic liquid electrolytes, J. Phys. Chem. B. 112 (2008) 12985–90. doi:10.1021/jp804097j.

[62] O. Borodin et al., Li^+ Cation Environment, Transport, and Mechanical Properties of the LiTFSI Doped N-Methyl-N-alkylpyrrolidinium$^+$TFSI$^-$ Ionic Liquids, J. Phys. Chem. B. 110 (2006) 16879–16886. doi:10.1021/jp061930t.

[63] S.-Y.Y. Lee et al., Two-cation competition in ionic-liquid-modified electrolytes for lithium ion batteries, J. Phys. Chem. B. 109 (2005) 13663–7. doi:10.1021/jp051974m.

[64] M. Yamagata et al., Charge–discharge behavior of graphite negative electrodes in bis(fluorosulfonyl)imide-based ionic liquid and structural aspects of their electrode/electrolyte interfaces, Electrochim. Acta 110 (2013) 181–190. doi:10.1016/j.electacta.2013.03.018.

[65] S. Xiong et al., Analysis of the solid electrolyte interphase formed with an ionic liquid electrolyte for lithium-sulfur batteries, J. Power Sources 252 (2014) 150–155. doi:10.1016/j.jpowsour.2013.11.119.

[66] B. Garcia et al., Room temperature molten salts as lithium battery electrolyte, Electrochim. Acta 49 (2004) 4583–4588. doi:10.1016/j.electacta.2004.04.041.

[67] A.I. Bhatt et al., Application of the N-propyl-N-methyl-pyrrolidinium Bis(fluorosulfonyl)imide RTIL Containing Lithium Bis(fluorosulfonyl)imide in Ionic Liquid Based Lithium Batteries, J. Electrochem. Soc. 157 (2010) A66. doi:10.1149/1.3257978.

[68] S. Fang et al., New functionalized ionic liquids based on pyrrolidinium and piperidinium cations with two ether groups as electrolytes for lithium battery, J.

Power Sources 196 (2011) 5637–5644. doi:10.1016/j.jpowsour.2011.02.047.

[69] D.R. MacFarlane et al., Energy applications of ionic liquids, Energy Environ. Sci. 7 (2014) 232–250. doi:10.1039/c3ee42099j.

[70] J.P. Salminen et al., Studies of Ionic Liquids in Lithium-Ion Battery Test Systems, ECS Trans. 1 (2006) 107–118. doi:10.1149/1.2209363.

[71] C. Liu et al., Ionic liquid electrolyte of lithium bis(fluorosulfonyl)imide/N-methyl-N-propylpiperidinium bis(fluorosulfonyl)imide for Li/natural graphite cells: Effect of concentration of lithium salt on the physicochemical and electrochemical properties, Electrochim. Acta 149 (2014) 370–385. doi:10.1016/j.electacta.2014.10.048.

[72] H. Matsumoto et al., Fast cycling of Li/$LiCoO_2$ cell with low-viscosity ionic liquids based on bis(fluorosulfonyl)imide $[FSI]^-$, J. Power Sources 160 (2006) 1308–1313. doi:10.1016/j.jpowsour.2006.02.018.

[73] T. Sugimoto et al., Ionic liquid electrolyte systems based on bis(fluorosulfonyl)imide for lithium-ion batteries, J. Power Sources 189 (2009) 802–805. doi:10.1016/j.jpowsour.2008.07.053.

[74] S. Seki et al., Compatibility of N-Methyl-N-propylpyrrolidinium Cation Room-Temperature Ionic Liquid Electrolytes and Graphite Electrodes, J. Phys. Chem. C. 112 (2008) 16708–16713. doi:10.1021/jp805403e.

[75] J. Li et al., Improved electrochemical performance of $LiMO_2$ (M=Mn, Ni, Co)–Li_2MnO_3 cathode materials in ionic liquid-based electrolyte, J. Power Sources 239 (2013) 490–495. doi:10.1016/j.jpowsour.2013.04.015.

[76] R.S. Kühnel et al., Anodic stability of aluminum current collectors in an ionic liquid based on the (fluorosulfonyl)(trifluoromethanesulfonyl)imide anion and its implication on high voltage supercapacitors, Electrochem. Commun. 38 (2014) 117–119. doi:10.1016/j.elecom.2013.11.014.

[77] X. Lin et al., Thermally-responsive, nonflammable phosphonium ionic liquid electrolytes for lithium metal batteries: operating at 100 degrees Celsius, Chem. Sci. (2015) 6601–6606. doi:10.1039/C5SC01518A.

[78] M. Schmidt et al., Lithium fluoroalkylphosphates: A new class of conducting salts for electrolytes for high energy lithium-ion batteries, J. Power Sources 97-98 (2001) 557–560. doi:10.1016/S0378-7753(01)00640-1.

[79] E. Peled, An Advanced Tool for the Selection of Electrolyte Components for Rechargeable Lithium Batteries, J. Electrochem. Soc. 145 (1998) 3482. doi:10.1149/1.1838831.

[80] S.E. Sloop et al., Chemical Reactivity of PF_5 and $LiPF_6$ in Ethylene

Carbonate/Dimethyl Carbonate Solutions, Electrochem. Solid-State Lett. 4 (2001) A42. doi:10.1149/1.1353158.

[81] U. Heider et al., Challenge in manufacturing electrolyte solutions for lithium and lithium ion batteries quality control and minimizing contamination level, J. Power Sources 81-82 (1999) 119–122. doi:10.1016/S0378-7753(99)00142-1.

[82] Y. Xia et al., Capacity Fading on Cycling of 4 V Li/$LiMn_2O_4$ Cells, J. Electrochem. Soc. 144 (1997) 2593. doi:10.1149/1.1837870.

[83] Z. Chen et al., $LiPF_6$/LiBOB blend salt electrolyte for high-power lithium-ion batteries, Electrochim. Acta 51 (2006) 3322–3326. doi:10.1016/j.electacta.2005.09.027.

[84] A.M. Andersson et al., The influence of lithium salt on the interfacial reactions controlling the thermal stability of graphite anodes, Electrochim. Acta 47 (2002) 1885–1898. doi:10.1016/S0013-4686(02)00044-0.

[85] J.T. Dudley et al., Conductivity of electrolytes for rechargeable lithium batteries, J. Power Sources 35 (1991) 59–82. doi:10.1016/0378-7753(91)80004-H.

[86] K. Zaghib et al., An improved high-power battery with increased thermal operating range: C-$LiFePO_4$//C-$Li_4Ti_5O_{12}$, J. Power Sources 216 (2012) 192–200. doi:10.1016/j.jpowsour.2012.05.025.

[87] M. Dahbi et al., Comparative study of EC/DMC LiTFSI and $LiPF_6$ electrolytes for electrochemical storage, J. Power Sources 196 (2011) 9743–9750. doi:10.1016/j.jpowsour.2011.07.071.

[88] L.J. Krause et al., Corrosion of aluminum at high voltages in non-aqueous electrolytes containing perfluoroalkylsulfonyl imides; new lithium salts for lithium-ion cells, J. Power Sources 68 (1997) 320–325. doi:10.1016/S0378-7753(97)02517-2.

[89] M. Morita et al., Anodic behavior of aluminum in organic solutions with different electrolytic salts for lithium ion batteries, Electrochim. Acta 47 (2002) 2787–2793. doi:http://dx.doi.org/10.1016/S0013-4686(02)00164-0.

[90] L. Péter et al., Anodic dissolution of aluminium in organic electrolytes containing perfluoroalkylsulfonyl imides, J. Appl. Electrochem. 29 (1999) 1053–1061. doi:10.1023/A:1003573430989.

[91] X. Chen et al., Mixed salts of LiTFSI and LiBOB for stable $LiFePO_4$-based batteries at elevated temperatures, J. Mater. Chem. A. 2 (2014) 2346. doi:10.1039/c3ta13043f.

[92] K. Matsumoto et al., Suppression of aluminum corrosion by using high concentration LiTFSI electrolyte, J. Power Sources 231 (2013) 234–238.

doi:10.1016/j.jpowsour.2012.12.028.

[93] D. Di Censo et al., Non-corrosive electrolyte compositions containing perfluoroalkylsulfonyl imides for high power Li-ion batteries, Electrochem. Commun. 7 (2005) 1000–1006. doi:http://dx.doi.org/10.1016/j.elecom.2005.07.005.

[94] B. Garcia et al., Aluminium corrosion in room temperature molten salt, J. Power Sources 132 (2004) 206–208. doi:10.1016/j.jpowsour.2003.12.046.

[95] E. Paillard et al., Electrochemical and Physicochemical Properties of $PY_{14}FSI$-Based Electrolytes with LiFSI, J. Electrochem. Soc. 156 (2009) A891. doi:10.1149/1.3208048.

[96] L. Li et al., Transport and Electrochemical Properties and Spectral Features of Non-Aqueous Electrolytes Containing LiFSI in Linear Carbonate Solvents, J. Electrochem. Soc. 158 (2011) A74–A82. doi:10.1149/1.3514705.

[97] Y. Deguchi et al., An advanced ionic liquid-lithium salt electrolyte mixture based on the bis(fluoromethanesulfonyl)imide anion, Electrochem. Commun. 43 (2014) 5–8. doi:10.1016/j.elecom.2014.02.017.

[98] H.-B. Han et al., Lithium bis(fluorosulfonyl)imide (LiFSI) as conducting salt for nonaqueous liquid electrolytes for lithium-ion batteries: Physicochemical and electrochemical properties, J. Power Sources 196 (2011) 3623–3632. doi:10.1016/j.jpowsour.2010.12.040.

[99] B. Philippe et al., Improved performance of nano-silicon electrodes using the salt LiFSI – A photoelectron spectroscopy study, J. Am. Chem. Soc. 135 (2013) 9829–9842. doi:10.1021/ja403082s.

[100] M. Nie et al., Role of Lithium Salt on Solid Electrolyte Interface (SEI) Formation and Structure in Lithium Ion Batteries, J. Electrochem. Soc. 161 (2014) A1001–A1006. doi:10.1149/2.054406jes.

[101] K. Kubota et al., Novel inorganic ionic liquids possessing low melting temperatures and wide electrochemical windows: Binary mixtures of alkali bis(fluorosulfonyl)amides, Electrochem. Commun. 10 (2008) 1886–1888. doi:10.1016/j.elecom.2008.10.001.

[102] S. Shui Zhang, An unique lithium salt for the improved electrolyte of Li-ion battery, Electrochem. Commun. 8 (2006) 1423–1428. doi:10.1016/j.elecom.2006.06.016.

[103] U. Wietelmann et al., Lithium bisoxalatoborate, the production thereof and its use as a conducting salt, US 6,506,516 B1, 1999.

[104] K. Xu et al., Lithium Bis(oxalato)borate Stabilizes Graphite Anode in

Propylene Carbonate, Electrochem. Solid-State Lett. 5 (2002) A259–A262.

[105] K. Xu et al., LiBOB: Is it an alternative salt for lithium ion chemistry?, J. Power Sources 146 (2005) 79–85. doi:10.1016/j.jpowsour.2005.03.153.

[106] X. Zhang et al., Passivation of Aluminum in Lithium-Ion Battery Electrolytes with LiBOB, J. Electrochem. Soc. 153 (2006) B365. doi:10.1149/1.2218269.

[107] K. Xu, Tailoring Electrolyte Composition for LiBOB, J. Electrochem. Soc. 155 (2008) A733. doi:10.1149/1.2961055.

[108] W.A. Henderson, Nonaqueous Electrolytes: Advances in Lithium Salts, in: R. Jow, K. Xu, O. Borodin, UeMakoto (Eds.), Electrolytes Lithium Lithium-Ion Batter., Springer, 2014: pp. 1–92.

[109] G.W.H. Höhne et al., Differential Scanning Calorimetry, Springer Berlin Heidelberg, Berlin, Heidelberg, 2003. doi:10.1007/978-3-662-06710-9.

[110] P. Haines, Principles of Thermal Analysis and Calorimetry, Royal Society of Chemistry, Cambridge, 2002. doi:10.1039/9781847551764.

[111] R.N.P. Choudhary et al., Materials Science and Technologies : Dielectric Materials : Introduction, Research and Applications, Nova Science Publishers, Inc., 2009.

[112] K. Hayamizu et al., Ionic conduction and ion diffusion in binary room-temperature ionic liquids composed of EMIMBF$_4$ and LiBF$_4$, J. Phys. Chem. B. 108 (2004) 19527–19532.

[113] B. Schrader, ed., Infrared and Raman Spectroscopy, Wiley-VCH Verlag GmbH, Weinheim, Germany, 1995. doi:10.1002/9783527615438.

[114] C. V. Raman et al., A New Type of Secondary Radiation, Nature 121 (1928) 501–502. doi:10.1038/121501c0.